

Over the past several decades, quantum information science has emerged to seek answers to the question: can we gain some advantage by storing, transmitting and processing information encoded in systems that exhibit unique quantum properties? Today it is understood that the answer is yes, and many research groups around the world are working towards the highly ambitious technological goal of building a quantum computer, which would dramatically improve computational power for particular tasks. A number of physical systems, spanning much of modern physics, are being developed for quantum computation. However, it remains unclear which technology, if any, will ultimately prove successful. Here we describe the latest developments for each of the leading approaches and explain the major challenges for the future.

In the past decade, there has been tremendous progress in the experimental development of a quantum computer: a machine that would exploit the full complexity of a many-particle quantum wavefunction to solve a computational problem. The context for the development of quantum computers may be clarified by comparison to a more familiar quantum technology: the laser. Before the invention of the laser we had technological advances in making light: fire, the lantern, the lightbulb. Until the laser, however, this light was always 'incoherent', meaning that the many electromagnetic waves generated by the source were emitted at completely random times with respect to each other. Quantum mechanical effects, however, allow these waves to be generated in phase, and the light source engineered to exploit this concept was the laser. Lasers are routine devices today, but they do not replace light bulbs for most applications. Their different kind of light—coherent light—is useful for thousands of applications from eye surgery to toys for cats, most of which were unimagined by the first laser physicists. Likewise, a quantum computer will not be a faster, bigger or smaller version of an ordinary computer. Rather, it will be a different kind of computer, engineered to control coherent quantum mechanical waves for different applications.

The example task for quantum computers which has provided the foremost motivation for their development is Shor's quantum algorithm for factoring large numbers<sup>1</sup>. This is one among several quantum algorithms that would allow modestly sized quantum computers to outperform the largest classical supercomputers in solving some specific problems important for data encryption. In the long term, another application may have higher technological impact: Feynman's 1980s proposal of using quantum computers for the efficient simulation of quantum systems<sup>1</sup>. Quantum mechanics will play an ever more important part in the behaviour of many emerging forms of artificial nanotechnology, and in our understanding of the nanomachinery of biological molecules. The engineering of the ultra-small will continue to advance and change our world in coming decades, and as this happens we might use quantum computers to understand and engineer such technology at the atomic level.

Quantum information research promises more than computers, as well. Similar technology allows quantum communication, which enables the sharing of secrets with security guaranteed by the laws

of physics. It also allows quantum metrology, in which distance and time could be measured with higher precision than is possible otherwise. The full gamut of potential technologies has probably not yet been imagined, nor will it be until actual quantum information hardware is available for future generations of quantum engineers.

Quantum computing 'software' is discussed elsewhere, such as in ref. 1. The central question of this review is what form quantum 'hardware' will take, and for this there are no easy answers. There are many possible materials for lasers — crystals, organic dye molecules, semiconductors, free electrons — and likewise there are many materials under consideration for quantum computers. Quantum bits are often imagined to be constructed from the smallest form of matter, an isolated atom, as in ion traps and optical lattices, but they may likewise be made far larger than routine electronic components, as in some superconducting systems. Only a few common features tie together the different hardware implementations of quantum computers currently under consideration, which we now describe.

### Requirements for quantum computing

Perhaps the most critical, universal aspect of quantum computers is the 'closed box' requirement: a quantum computer's internal operation, while under the programmer's control, must otherwise be isolated from the rest of the Universe. Small amounts of information leakage from the box can disturb the fragile quantum mechanical waves on which the quantum computer depends, causing the quantum mechanically destructive process known as decoherence.

Decoherence comes in several forms. Quantum mechanical waves—such as light from a laser, or the oscillations of the constituents in quantum computers—show interference phenomena, but these phenomena vanish in repeated trial experiments because, owing to various processes, phases no longer 'cohere' after a certain time. In an ensemble measurement, trial-to-trial variations in oscillator frequency lead to an apparent damping of wave interference on a timescale called  $T_2^*$ , illustrated in Fig. 1a. A single trial of a single quantum oscillator might retain its phase coherence for a much longer time than  $T_2^*$ . Eventually, random processes add or subtract energy from the oscillator, bringing the system to thermal equilibrium on a timescale called  $T_1$ . Processes may also only 'borrow' energy from the environment, thus changing

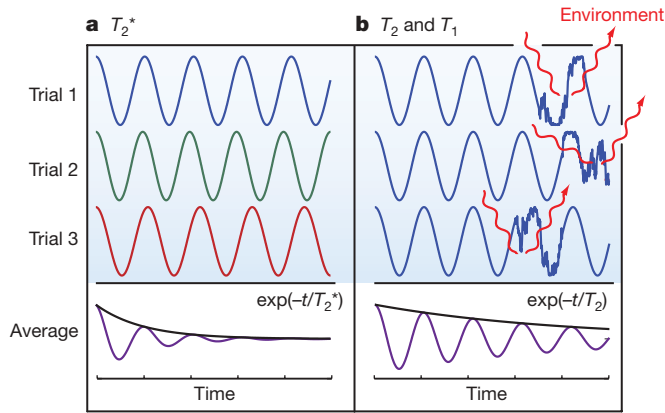


**Figure 1 | Dephasing and decoherence.** **a**, An oscillator with frequency varying by trial, as indicated by the differently coloured waves, averages to an oscillation decaying with apparent dephasing timescale  $T_2^*$ . **b**, A quantum oscillator interacting with the environment may have phase-kicks in a single trial; these are the processes that harm coherence in quantum computation, and lead to an average decay process of timescale  $T_2$ . Equilibration processes are similar, and cause decay on the timescale  $T_1 \geq T_2/2$ .

the oscillator’s phase, causing oscillations to damp on a timescale called  $T_2$ , as illustrated in Fig. 1b. Fundamentally  $T_2 \leq 2T_1$ , and for most systems  $T_1 \gg T_2$ , which means that  $T_2$  is more important for quantum computation.

No system is fully free of decoherence, but small amounts of decoherence may be removed through various techniques gathered under the name of ‘quantum error correction’ (QEC). Moreover, errors in quantum computers can be corrected using error-prone resources; that is, they may be made fault-tolerant<sup>1</sup> for error probabilities beneath a critical threshold that depends on the computer hardware, the sources of error, and the protocols used for QEC. Realistically, most of the resources used in a fault-tolerant quantum computer will be in place to correct its own errors. If computational resources are unconstrained, the fault-tolerant threshold might be as high as 3% (ref. 2); values estimated under typical constraints are much smaller, on the order of  $10^{-5}$ . The value of  $T_2$  is used as an initial characterization of many quantum systems, since, at a bare minimum, elements of a quantum computer need to be operated much faster than  $T_2$  to allow fault-tolerance. However, other types of errors are just as important, and a large system often exhibits correlated noise processes distinct from  $T_2$  decoherence.

An early characterization of the physical requirements for an implementation of a fault-tolerant quantum computer was carried out by DiVincenzo<sup>3</sup>. A long  $T_2$  is the third of these criteria, but this raises the question: what criteria must  $T_2$  be long enough to satisfy? Since DiVincenzo’s seminal work, the ideas for implementing quantum computing have diversified, and the DiVincenzo criteria as originally stated are difficult to apply to many emerging concepts. Here, we rephrase DiVincenzo’s original considerations into three more general criteria; these are stated with the assumption that they are achievable while keeping decoherence ‘small enough’.

**Scalability.** The computer must operate in a Hilbert space whose dimensions can grow exponentially without an exponential cost in resources (such as time, space or energy).

The standard way to achieve this follows the first DiVincenzo criterion: one may simply add well-characterized qubits to a system. A quantum system with two states, such as a quantum spin with  $S = 1/2$ , is a qubit. A qubit in a superposition of its two states is a quantum oscillator, and it inevitably experiences some amount of  $T_1$  and  $T_2$  relaxation. A single qubit could be emulated by a classical oscillator with a randomly timed, single-bit read-out, but quantum mechanics also allows entanglement. As a result, the logic space potentially available on a quantum system of  $N$  qubits is described by a very large group [known as  $SU(2^N)$ ], which is much larger than

the comparable group  $[SU(2)^{\otimes N}]$  of  $N$  unentangled spins, and cannot be emulated by  $N$  classical oscillators or  $N$  classical bits. Ultimately, it is the large Hilbert space of a quantum computer that allows it operations unavailable to classical computers. For qubits, the size and energy of a quantum computer generally grows linearly with  $N$ . But qubits are not a prerequisite; quantum  $d$ -state systems (qudits) or quantum continuous variables may also enable quantum computation.

Declaring a technology ‘scalable’ is a tricky business, because the resources used to define and control a qubit are diverse. They may include space on a microchip, classical microwave electronics, dedicated lasers, cryogenic refrigerators, and so on. For a system to be scalable, these ‘classical’ resources must be made scalable as well, which invokes complex engineering issues and the infrastructure available for large-scale technologies.

**Universal logic.** The large Hilbert space must be accessible using a finite set of control operations; the resources for this set must also not grow exponentially.

In the standard picture of quantum computing, this criterion (DiVincenzo’s fourth) requires a system to have available a universal set of quantum logic gates. In the case of qubits, it is sufficient to have available nearly ‘analogue’ single-qubit gates (for example, arbitrary rotations of a spin-qubit), and almost any one ‘digital’ two-qubit entangling logic operation, such as the controlled-NOT gate.

But quantum computers need not be made with gates. In adiabatic quantum computation<sup>4</sup>, one defines the answer to a computational problem as the ground state of a complex network of interactions between qubits, and then one adiabatically evolves those qubits into that ground state by slowly turning on the interactions. In this case, evaluation of this second criterion requires that one must ask whether the available set of interactions is complex enough, how long it takes to turn on those interactions, and how cold the system must be kept. As another example, in cluster-state quantum computation<sup>5</sup>, one particular quantum state (the cluster state) is generated in the computer through a very small set of non-universal quantum gates, and then computation is performed by changing the way in which the resulting wavefunction is measured. The qubits can be measured in arbitrary bases to provide the ‘analogue’ component that completes the universal logic. Adiabatic and cluster-state quantum computers are equivalent in power to gate-based quantum computers<sup>4</sup>, but their implementation may be simpler for some technologies.

**Correctability.** It must be possible to extract the entropy of the computer to maintain the computer’s quantum state.

Any QEC protocol will require some combination of efficient initialization (DiVincenzo’s second criterion) and measurement (DiVincenzo’s fifth criterion) to flush unwanted entropy introduced from the outside world out of the computer. Initialization refers to the ability to cool a quantum system quickly into a low-entropy state; for example, the polarization of a spin into its ground state. Measurement refers to the ability to determine the state of a quantum system quickly with the accuracy allowed by quantum mechanics. In some situations, these two abilities are the same. For example, a quantum non-demolition (QND) measurement alters the quantum state by projecting to the measured state, which remains the same even after repeated measurements. Performing a QND measurement also initializes the quantum system into the measured state. The relationship between the need for initialization and measurement in QEC is complex; one may generally be replaced by the other. Of course, some form of measurement is always needed to read out the state of the computer at the end of a computation, and some amount of physical initialization is needed at the beginning, but how much is needed is unclear; schemes have been developed to allow some forms of quantum computation with states of high entropy<sup>6–9</sup>.

Quantum computation is difficult because the three basic criteria we have discussed appear to be in conflict. For example, those parts of the system in place to achieve rapid measurement must be turned strongly ‘on’ for error correction and read-out, but must be turned strongly ‘off’

to preserve the coherences in the large Hilbert space. Generally, neither the ‘on’ state nor the ‘off’ state is as difficult to implement as the ability to switch between the two! In engineering a scalable quantum computer architecture, these conflicts are often aided by techniques for quantum communication; for this DiVincenzo introduced extra criteria related to the ability to convert stationary qubits to ‘flying qubits’ such as photons. Quantum communication allows small quantum computers to be ‘wired together’ to make larger ones, it allows specialized measurement hardware to be located distantly from sensitive quantum memories, and it makes it easier to achieve the strong qubit connectivity required by most schemes for fault-tolerance.

The central challenge in actually building quantum computers is maintaining the simultaneous abilities to control quantum systems, to measure them, and to preserve their strong isolation from uncontrolled parts of their environment. In the ensuing sections, we introduce the various technologies researchers are currently employing to meet this challenge.

## Photons

Realizing a qubit as the polarization state of a photon is appealing because photons are relatively free of the decoherence that plagues other quantum systems. Polarization rotations (one-qubit gates) can easily be done using ‘waveplates’ made of birefringent material. (Photons also allow the encoding of a qubit on the basis of location and timing; quantum information may also be encoded in the continuous phase and amplitude variables of many-photon laser beams<sup>10</sup>.) However, achieving the needed interactions between photons for universal multi-qubit control presents a major hurdle. The necessary interactions appear to require optical nonlinearities stronger than those available in conventional nonlinear media, and initially it was believed that electromagnetically induced transparency<sup>11</sup> or atom–photon interactions enhanced by an optical cavity (cavity quantum electrodynamics)<sup>12</sup> would be required.

In 2001, a breakthrough known as the KLM (Knill–Laflamme–Milburn<sup>13</sup>) scheme showed that scalable quantum computing is possible using only single-photon sources and detectors, and linear optical circuits. This scheme relies on quantum interference with auxiliary photons at a beamsplitter and single-photon detection to induce interactions nondeterministically. In the past five years, the KLM scheme has moved from a mathematical proof-of-possibility towards practical realization, with demonstrations of simple quantum algorithms<sup>14</sup> and theoretical developments that dramatically reduce the resource overhead<sup>15</sup>. These developments employ the ideas of cluster-state quantum computing<sup>5</sup>, and have been demonstrated experimentally<sup>15</sup>. Today, efforts are focused on high-efficiency single-photon detectors<sup>16,17</sup> and sources<sup>18,19</sup>, devices that would enable a deterministic interaction between photons<sup>11,12</sup>, and chip-scale waveguide quantum circuits<sup>14,20</sup>.

Silicon single-photon detectors operate at room temperature at 10 MHz with 70% efficiency; work is in progress to increase efficiency and to resolve the photon number<sup>16,17</sup>. Superconducting detectors operating as sensitive thermometers can resolve the photon number, have 95% efficiency and low noise, but operate at  $\sim 100$  mK and are relatively slow. Faster (hundreds of MHz) nanostructured NbN superconducting nanowire detectors have achieved high efficiency and photon number resolution<sup>16,17</sup>.

One approach to a high-efficiency single-photon source is to multiplex the nonlinear optical sources currently used to emit pairs of photons spontaneously<sup>18</sup>. An alternative is a single quantum system in an optical cavity that emits a single photon on transition from an excited to a ground state. Robust alignment of the cavity can be achieved with solid-state ‘artificial atoms’, such as quantum dots<sup>18,19,21,22</sup> and potentially with impurities in diamond<sup>23</sup>, which we discuss below. As these cavity quantum electrodynamics systems improve, they could provide deterministic photon–photon nonlinearities<sup>24</sup>.

Regardless of the approach used for photon sources, detectors and nonlinearities, photon loss remains a significant challenge, and

**Table 1 | Current performance of various qubits**

Type of qubit	$T_2$	Benchmarking (%)		References
		One qubit	Two qubits	
Infrared photon	0.1 ms	0.016	1	20
Trapped ion	15 s	0.48 <sup>†</sup>	0.7*	104–106
Trapped neutral atom	3 s	5		107
Liquid molecule nuclear spins	2 s	0.01 <sup>†</sup>	0.47 <sup>†</sup>	108
$e^-$ spin in GaAs quantum dot	3 $\mu$ s	5		43, 57
$e^-$ spins bound to $^{31}\text{P}$ - $^{28}\text{Si}$	0.6 s	5		49
$^{29}\text{Si}$ nuclear spins in $^{28}\text{Si}$	25 s	5		50
NV centre in diamond	2 ms	2	5	60, 61, 65
Superconducting circuit	4 $\mu$ s	0.7 <sup>†</sup>	10*	73, 79, 81, 109

Measured  $T_2$  times are shown, except for photons where  $T_2$  is replaced by twice the hold-time (comparable to  $T_1$ ) of a telecommunication-wavelength photon in fibre. Benchmarking values show approximate error rates for single or multi-qubit gates. Values marked with asterisks are found by quantum process or state tomography, and give the departure of the fidelity from 100%. Values marked with daggers are found with randomized benchmarking<sup>10</sup>. Other values are rough experimental gate error estimates. In the case of photons, two-qubit gates fail frequently but success is heralded; error rates shown are conditional on a heralded success. NV, nitrogen vacancy.

provides the closest comparison to  $T_2$  decoherence in matter-based qubits (see Table 1). Like decoherence, loss can be handled by QEC techniques with high thresholds<sup>15</sup>. Typical values for loss in integrated waveguide devices are  $\sim 0.1$  dB  $\text{cm}^{-1}$ . Current silica waveguide circuits<sup>14</sup> use about one centimetre per logic gate (see Fig. 2), a length which may be reduced by using circuits with higher refractive-index contrast. The advances in photonic quantum computing not only support photonic qubits, but are likely to benefit other types of quantum computer hardware using photons for quantum communication between matter qubits, including trapped atoms, quantum dots and solid-state dopants, as discussed below.

## Trapped atoms

The best time and frequency standards are based on isolated atomic systems, owing to the excellent coherence properties of certain energy levels within atoms. Likewise, these energy levels in trapped atoms form very reliable qubits, with  $T_1$  and  $T_2$  times typically in the range of seconds and longer. Entangling quantum gates can be realized through appropriate interactions between atoms, and atomic qubits can be initialized by optical pumping and measured with nearly 100% efficiency through the use of state-dependent optical fluorescence detection.

Individual atomic ions can be confined in free space with nanometre precision using appropriate electric fields from nearby electrodes<sup>25,26</sup>, as shown in Fig. 3a and b. Multiple trapped ion qubits can be entangled through a laser-induced coupling of the spins mediated by a collective mode of harmonic motion in the trap. The simplest realization of this interaction to form entangling quantum gates was first proposed by Cirac and Zoller in 1995 and demonstrated in the laboratory later that year<sup>25</sup>. Extensions to this approach rely on optical spin-dependent forces that do not require individual optical addressing of the ions, nor the preparation of the ionic motion into a

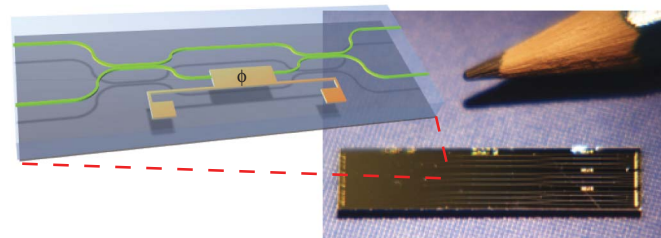


**Figure 2 | Photonic quantum computer.** A microchip containing several silica-based waveguide interferometers with thermo-optic controlled phase shifts for photonic quantum gates<sup>20</sup>. Green lines show optical waveguides; yellow components are metallic contacts. Pencil tip shown for scale.

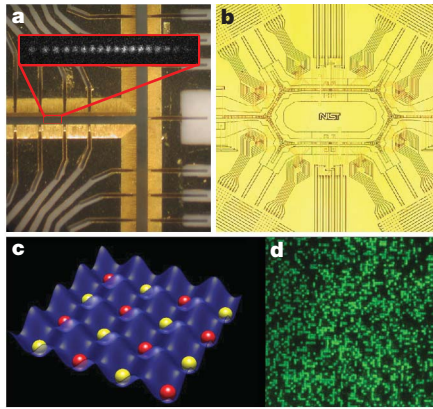


**Figure 3 | Trapped atom qubits.** **a**, Multi-level linear ion trap chip; the inset displays a linear crystal of several  $^{171}\text{Yb}^+$  ions fluorescing when resonant laser light is applied (the ion–ion spacing is  $4\ \mu\text{m}$  in the figure). Other lasers can provide qubit-state-dependent forces that can entangle the ions through their Coulomb interaction. **b**, Surface ion trap chip with 200 zones distributed above the central hexagonal racetrack of width  $2.5\ \text{mm}$  (photograph courtesy of J. Amini and D. J. Wineland). **c**, Schematic of optical lattice of cold atoms formed by multi-dimensional optical standing wave potentials (graphic courtesy of J. V. Porto). **d**, Image of individual Rb atoms from a Bose condensate confined in a two-dimensional optical lattice, with atom–atom spacing of  $0.64\ \mu\text{m}$  (photograph courtesy of M. Greiner).

pure quantum state, and are thus favoured in current experiments. Recently, up to eight trapped ion qubits have been entangled in this way<sup>26</sup>. There are also proposals to use radio-frequency magnetic field gradients<sup>27</sup> or ultrafast spin-dependent optical forces<sup>28</sup> that do not require the ions to be localized to within an optical wavelength (the Lamb–Dicke limit).

The scaling of trapped-ion Coulomb gates becomes difficult when large numbers of ions participate in the collective motion for several reasons: laser-cooling becomes inefficient, the ions become more susceptible to noisy electric fields and decoherence of the motional modes<sup>29</sup>, and the densely packed motional spectrum can potentially degrade quantum gates through mode crosstalk and nonlinearities<sup>25</sup>. In one promising approach to circumvent these difficulties, individual ions are shuttled between various zones of a complex trap structure through the application of controlled electrical forces from the trap electrodes. In this way, entangling gates need only operate with a small number of ions<sup>30</sup>.

Another method for scaling ion trap qubits is to couple small collections of Coulomb-coupled ions through photonic interactions, offering the advantage of having a communication channel that can easily traverse large distances. Recently, atomic ions have been entangled over macroscopic distances in this way<sup>31</sup>. This type of protocol is similar to probabilistic linear optics quantum computing schemes discussed above<sup>13</sup>, but the addition of stable qubit memories in the network allows the system to be efficiently scaled to long-distance communication through quantum repeater circuits<sup>32</sup>. Moreover, such a system can be scaled to large numbers of qubits for distributed probabilistic quantum computing<sup>33</sup>.

Neutral atoms provide qubits similar to trapped ions. An array of cold neutral atoms may be confined in free space by a pattern of crossed laser beams, forming an optical lattice<sup>34</sup>. The lasers are typically applied far from atomic resonance, and the resulting Stark shifts in the atoms provide an effective external trapping potential for the atoms. Appropriate geometries of standing-wave laser beams can result in a regular pattern of potential wells in one, two or three dimensions, with the lattice-site spacing scaled by the optical wavelength (Fig. 3c, d). Perhaps the most intriguing aspect of optical lattices is that the dimensionality, form, depth and position of optical lattices can be precisely controlled through the geometry, polarization and intensity of the external laser beams defining the lattice. The central challenges in using

optical lattices for quantum computing are the controlled initialization, interaction and measurement of the atomic qubits. However, there has been much progress on all of these fronts in recent years.

Optical lattices are typically loaded with  $10^3$ – $10^6$  identical atoms, usually with non-uniform packing of lattice sites for thermal atoms. However, when a Bose condensate is loaded in an optical lattice, the competition between intrasite tunnelling and the on-site interaction between multiple atoms can result in a Mott-insulator transition where approximately the same number of atoms (for example, one) reside in every lattice site<sup>34</sup>. The interaction between atomic qubits in optical lattices can be realized in several ways. Adjacent atoms can be brought together depending on their internal qubit levels with appropriate laser forces, and through contact interactions, entanglement can be formed between the atoms. This approach has been exploited for the realization of entangling quantum gate operations between atoms and their neighbours<sup>35</sup>. Another approach exploits the observation that when atoms are promoted to Rydberg states, they possess very large electric dipole moments. The Rydberg ‘dipole blockade’ mechanism prevents more than one atom from being promoted to a Rydberg state, owing to the induced level shift of the Rydberg state in nearby atoms. Recently, the Rydberg blockade was used to entangle two atoms confined in two separate optical dipole traps<sup>36,37</sup>, and it should be possible to observe this between many more atoms in an optical lattice.

For trapped atoms and ions, coherence times are many orders of magnitude longer than initialization, multi-qubit control, and measurement times. The critical challenge for the future of trapped atom quantum computers will be to preserve the high-fidelity control already demonstrated in small systems while scaling to larger, more complex architectures.

### Nuclear magnetic resonance

Nuclear spins in molecules in liquid solutions make excellent gyroscopes; rapid molecular motion actually helps nuclei maintain their spin orientation for  $T_2$  times of many seconds, comparable to coherence times for trapped atoms. In 1996, methods were proposed<sup>6,7</sup> for building small quantum computers using these nuclear spins in conjunction with 50 years’ worth of existing magnetic resonance technology.

Immersed in a strong magnetic field, nuclear spins can be identified through their Larmor frequency. In a molecule, nuclear Larmor frequencies vary from atom to atom owing to shielding effects from electrons in molecular bonds. Irradiating the nuclei with resonant radio-frequency pulses allows manipulation of nuclei of a distinct frequency, giving generic one-qubit gates. Two-qubit interactions arise from the indirect coupling mediated through molecular electrons. Measurement is achieved by observing the induced current in a coil surrounding the sample of an ensemble of such qubits.

Liquid-state nuclear magnetic resonance has allowed the manipulation of quantum processors with up to a dozen qubits<sup>38</sup>, and the implementation of algorithms<sup>39</sup> and QEC protocols. This work was enabled in large part by the development of quantum-information-inspired advances in radio-frequency pulse techniques building on the many years of engineering in magnetic resonance imaging and related technologies; these techniques continue to improve<sup>40</sup>.

Initialization is an important challenge for nuclear magnetic resonance quantum computers. The first proposals employed pseudo-pure-state techniques, which isolate the signal of an initialized pure state against a high-entropy background. However, the techniques first suggested were not scalable. Algorithmic cooling techniques<sup>8</sup> may help this problem in conjunction with additional nuclear polarization. It was also noticed that for small numbers of qubits, pseudo-pure-state-based computation may be shown to lack entanglement<sup>41</sup>. Investigations of the consequences of this issue spurred insight into the origin of the power of quantum computers and led to new models of quantum computation and algorithms<sup>9</sup>.

One way to address the scalability limitation of pseudo-pure states is to move to solid-state nuclear magnetic resonance, for which a

variety of dynamic nuclear polarization techniques exist. The lack of molecular motion allows the use of nuclear dipole–dipole couplings, which may speed up gates considerably. A recent example of a step towards solid-state nuclear magnetic resonance quantum computation can be found in the implementation of many rounds of heat-bath algorithmic cooling<sup>8</sup>. Another method of possibly extending solid-state nuclear magnetic resonance systems is to include electrons to assist in nuclear control<sup>42</sup>. These techniques have possible application to the solid-state dopants discussed in the next section.

To date, no bulk nuclear magnetic resonance technique has shown sufficient initialization or measurement capabilities for effective correctness, but nuclear magnetic resonance has led the way in many-qubit quantum control. The many-second  $T_2$  times are comparable to gate times in liquids and much longer than the sub-millisecond gate times in solids, but are still short in comparison to timescales for initialization and measurement. The many lessons learned in nuclear magnetic resonance quantum computation research are most likely to be relevant for advancing the development of other quantum technologies.

### Quantum dots and dopants in solids

A complication of quantum computing with single atoms in vacuum is the need to cool and trap them. Large arrays of qubits may be easier to assemble and cool if the ‘atoms’ are integrated into a solid-state host, motivating the use of quantum dots and single dopants in solids. These ‘artificial atoms’ occur when a small semiconductor nanostructure, impurity or impurity complex binds one or more electrons or holes (empty valence-band states) into a localized potential with discrete energy levels, which is analogous to an electron bound to an atomic nucleus.

Quantum dots come in many varieties. Some are electrostatically defined quantum dots, where the confinement is created by controlled voltages on lithographically defined metallic gates. Others are self-assembled quantum dots, where a random semiconductor growth process creates the potential for confining electrons or holes. A key difference between these two types of quantum dots is the depth of the atom-like potential they create; as a result electrostatically defined quantum dots operate at very low temperatures ( $< 1$  K) and are primarily controlled electrically, whereas self-assembled quantum dots operate at higher temperatures ( $\sim 4$  K) and are primarily controlled optically.

One of the earliest proposals for quantum computation in semiconductors, that of Loss and DiVincenzo, envisioned arrays of electrostatically defined dots, each containing a single electron whose two spin states provide a qubit. Quantum logic would be accomplished by changing voltages on the electrostatic gates to move electrons closer and further from each other, activating and deactivating the exchange interaction<sup>43</sup>.

The ‘spin-to-charge conversion’ needed for the measurement of single spins in quantum dots has since been demonstrated, using either a single-electron transistor or a quantum point contact. These devices exhibit a conductance sensitive to the charge of a single trapped electron in a nearby quantum dot. The single-electron transistor or quantum point contact thereby allows the measurement of a single electron charge; to measure a spin, the ability of a single electron to tunnel into or out of a quantum dot is altered according to its spin state<sup>43</sup>. The control of individual spins has also been demonstrated via direct generation of microwave magnetic and electric fields. These techniques have allowed measurement of  $T_2^*$  and  $T_2$  times by spin-echo techniques. Qubits may also be defined by clusters of exchange-coupled spins, with effective single-qubit logic controlled by the pairwise exchange interaction. Voltage control of a multi-electron qubit via the exchange interaction has the particular advantage of being faster than direct microwave transitions. The  $T_2$  decoherence of a qubit defined by an exchange-coupled electron pair was measured this way<sup>43</sup>.

A critical issue in the work described above, which was performed on dots made with group III–V semiconductors, is the inevitable presence of nuclear spins in the semiconductor substrate. Nuclear spins both create an inhomogeneous magnetic field, resulting in  $T_2^* \approx 10$  ns, and cause decoherence via dynamic spin-diffusion from the nuclear dipole–dipole interactions. This latter process limits electron spin decoherence times ( $T_2$ ) to a few microseconds<sup>43</sup>. Suppressing this decoherence requires either extraordinary levels of nuclear polarization, or the dynamic decoupling of nuclear spin noise by rapid sequences of spin rotations<sup>44</sup>.

One way to eliminate nuclear spins altogether is to use nuclear-spin-free group-IV semiconductors (that is, silicon and germanium). Many of the accomplishments demonstrated in GaAs have recently been duplicated in metal-oxide-semiconductor silicon-based<sup>45</sup> and SiGe-based quantum dots, including single electron charge sensing and the control of tunnel coupling in double dots<sup>46</sup>.

In related silicon-based proposals<sup>47,48</sup>, the quantum dot is replaced by a single impurity, in particular a single phosphorus atom, which binds a donor electron at low temperature. Quantum information may then be stored in either the donor electron, or in the state of the single  $^{31}\text{P}$  nuclear spin, accessed via the electron-nuclear hyperfine coupling. Phosphorus-bound electron spins in isotopically purified  $^{28}\text{Si}$  show encouragingly long  $T_2$  times exceeding 0.6 s, as demonstrated by electron-spin resonance<sup>49</sup>. The potential for nuclear spin decoherence times of minutes or longer has further been seen in nuclear magnetic resonance dynamic decoupling experiments<sup>50</sup> with  $^{29}\text{Si}$  in  $^{28}\text{Si}$ . Isotopically purified silicon also shows optical transitions related to the  $^{31}\text{P}$  donor that are extremely sharp in comparison to other optical solid-state systems, revealing inhomogeneous broadening comparable to the 60-MHz hyperfine coupling. These transitions enable rapid (less than 1 s) electron and nuclear spin polarization by optical pumping<sup>51</sup>. Recently, silicon-based transistors have aided the detection of the ion-implantation of single dopants<sup>52</sup>, a technique which adds to scanning tunnelling microscopy techniques<sup>53</sup> for placing phosphorus impurities in prescribed atomic locations.

However, a challenge in using electrostatically defined quantum dots or silicon-based impurities for quantum computation is that the exchange interaction is extremely short-range, imposing a substantial constraint when considering the requirements of fault-tolerant QEC. As with trapped ions and atoms, photonic connections between quantum dots may help to resolve this issue. Self-assembled quantum dots are particularly useful for these connections because their large size in comparison to single atoms increases their coupling to photons.

The development of self-assembled dots is hindered by their random nature; they form in random locations and, unlike atoms, their optical characteristics vary from dot to dot. Emerging fabrication techniques for deterministic placement of dots<sup>54</sup> and dot tuning techniques<sup>21,22</sup> may remedy this problem for future quantum computers. In the meantime, the optical control and measurement of qubits in self-assembled quantum dots has recently progressed. Rapid optical initialization has been demonstrated for both electrons and holes<sup>55–57</sup>. Optical QND measurements<sup>58</sup> and single-spin control via ultrafast pulses have been developed<sup>57</sup>. Remarkably, these qubits may be controlled very quickly, on the order of picoseconds, potentially enabling extremely fast quantum computers.

Optically active solid-state dopants also allow photonic connections, but with greater optical homogeneity. The negatively charged nitrogen-vacancy centre in diamond (Fig. 4c) is one such dopant. It consists of a substitutional nitrogen at a lattice site neighbouring a missing carbon atom. The negatively charged state of the nitrogen-vacancy centre forms a triplet spin system. Under optical illumination, spin-selective relaxations facilitate efficient optical pumping of the system into a single spin state, allowing fast (250 ns) initialization of the spin qubit<sup>59</sup>. The spin state of a nitrogen-vacancy centre may then be coherently manipulated with resonant microwave fields<sup>60</sup>, and then detected in a few milliseconds via spin-dependent

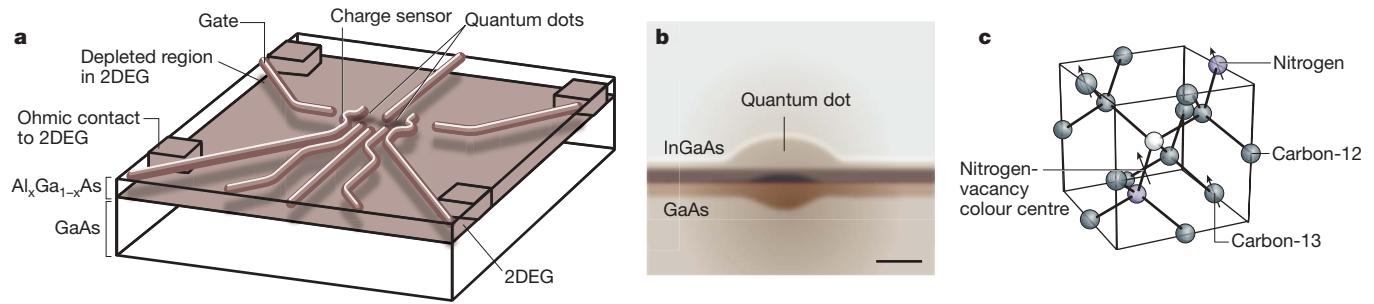


**Figure 4 | Quantum dot and solid-state dopant qubits.** **a**, An electrostatically confined quantum dot; the structure shown is several  $\mu\text{m}$  across. 2DEG, two-dimensional electron gas. **b**, A self-assembled quantum

fluorescence in an optical microscope<sup>23</sup>. As in silicon, the nuclear structure near the impurity is sufficiently clean to allow hyperfine-mediated nuclear spin memory<sup>60,61</sup>; this memory in turn may assist in electron-spin readout<sup>62</sup>.

Owing to a nearly nuclear-spin-free carbon lattice and low spin-orbit coupling, nitrogen-vacancy centres show longer spin coherence times than GaAs quantum dots, even at room temperature. In low-purity, technical-grade synthetic material, single substitutional nitrogen atoms cause major effects on the electronic spin properties of nitrogen-vacancy centres<sup>63</sup>. This electron spin bath can be polarized in high magnetic fields leading to a complete freezing of the nitrogen spin dynamics<sup>64</sup>. Decoherence times are much longer in ultrapure diamond. Recently, it was shown that a chemical vapour deposition process allows reduction of the impurity concentration down to about 0.1 parts per billion. In such materials, the nuclear spin bath formed by <sup>13</sup>C nuclei (natural abundance of about 1.1%) governs the dynamics of the electron spin of nitrogen-vacancy centres<sup>60</sup>. By growing isotopically enriched <sup>12</sup>C diamond, it is possible to increase  $T_2$  to 2 ms for 99.7% pure material. The  $T_1$  limit is expected to be of the order of seconds at room temperature<sup>65</sup>.

Magnetic interactions between quantum dots or dopant spins allow local couplings, as recently demonstrated in diamond<sup>66</sup>. Longer-distance optical connections between such qubits are likely to be strongly assisted by cavity quantum electrodynamics with optical microcavities. The critical figure of merit for the microcavity is the cooperativity parameter, which is proportional to the cavity quality factor  $Q$  divided by the cavity mode volume. The latter may be very small in solid-state microcavities, on the scale of the cube of the optical wavelength, leading to initial demonstrations of quantum logic between single, self-assembled quantum dots in high-cooperativity microcavities and single photons<sup>22</sup>. Microcavities will be especially important for nitrogen-vacancy centres<sup>67</sup>, because their zero-phonon emission line is weaker than for typical quantum dot transitions.

Other materials showing strong optical characteristics and nuclear-spin-free substrates are also under consideration. In diamond, nickel-related centres exhibit narrow-band, near-infrared emission at room temperature<sup>68</sup>, and silicon-vacancy defects are known to have a paramagnetic ground state similar to that in nitrogen-vacancy defects<sup>69</sup>. In the wide-gap, group II–VI semiconductor ZnSe, the fluorine impurity has a similar binding energy and spin structure to that of phosphorus in silicon and a comparable potential for isotopic depletion of nuclear spins from the substrate. Unlike silicon- or diamond-based impurities, it has an oscillator strength comparable to that of a quantum dot<sup>70</sup>.

Although it is routine to make large wafers of spins trapped in dots and impurities, scaling a system of coupled spins remains a challenge. The microsecond  $T_2$  times seen in GaAs are long in comparison to their 1–100-ps qubit control times and 1–10-ns measurement and

dot. Scale bar,  $\sim 5$  nm. **c**, The atomic structure of a nitrogen-vacancy centre in the diamond lattice, with lattice constant 3.6 Å. Figure copied from figure 1 of ref. 111 with permission.

initialization times, but large-scale systems will require improved connectivity and homogeneity. The longer, millisecond  $T_2$  times in the more homogeneous silicon and diamond systems must be considered alongside the slower, developing methods to couple these qubits.

### Superconductors

Qubits made from ordinary electrical circuits would decohere quickly owing to resistive power loss. In superconductors at low temperature, however, electrons bind into Cooper pairs that condense into a state with zero-resistance current and a well-defined phase. In superconducting circuits, the potential for the quantum variables of that Cooper-pair condensate may be changed by controlling macroscopically defined inductances ( $L$ ), capacitances ( $C$ ), and so on, allowing the construction of qubits. Likewise, the potential may be dynamically altered by electrical signals to give complete quantum control. These devices therefore resemble classical high-speed integrated circuits and can be readily fabricated using existing technologies.

The basic physics behind superconducting qubits is most easily explained by analogy to the simpler quantum mechanical system of a single particle in a potential. To begin, an ordinary  $LC$ -resonator circuit provides a quantum harmonic oscillator. The magnetic flux across the inductor  $\Phi$  and the charge on the capacitor plate  $Q$  have the commutator  $[\Phi, Q] = i\hbar$ , and therefore  $\Phi$  and  $Q$  are respectively analogous to the position and momentum of a single quantum particle. The dynamics are determined by the ‘potential’ energy  $\Phi^2/2L$  and the ‘kinetic’ energy  $Q^2/2C$ , which results in the well-known equidistant level quantization of the harmonic oscillator. However, anharmonicity is needed, and it is available from the key component in superconducting qubits: the Josephson junction. A Josephson junction is a thin insulating layer separating sections of a superconductor. The quantization of the tunnelling charge across the junction brings a cosine term to the parabola in the potential energy with an amplitude given by the Josephson energy  $E_J$ , which is proportional to the junction critical current. Two of the quantized levels in the resulting anharmonic potential give rise to a qubit.

There are three basic types of superconducting qubits—charge, flux and phase—with potentials shown in Fig. 5b–d. A critical difference between the different qubit types is the ratio  $E_J/E_C$ , where  $E_C = e^2/2C$  is the single electron charging energy characterizing the charging effect, that is, the kinetic term. This ratio alters the nature of the wavefunctions and their sensitivity to charge and flux fluctuations.

The first type of superconducting qubit, the charge qubit, omits the inductance. There is no closed superconducting loop, and the potential is simply a cosine with a minimum at zero phase. It is sometimes called a Cooper-pair box, because it relies ultimately on the quantization of charge into individual Cooper pairs, which becomes a dominant effect when a sufficiently small ‘box’ electrode

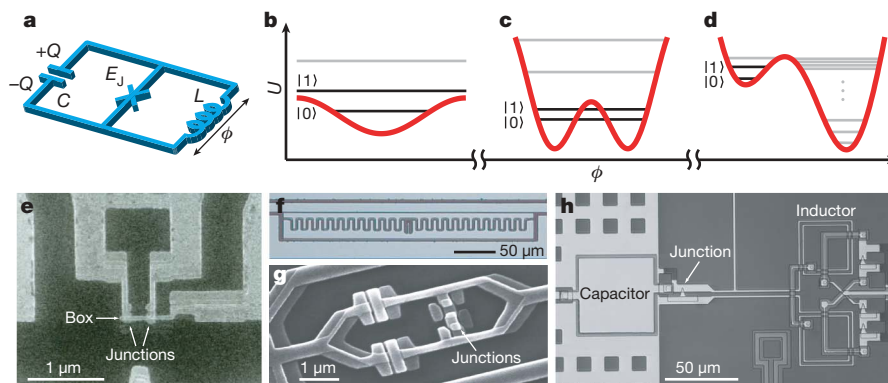


**Figure 5 | Superconducting qubits.** **a**, Minimal circuit model of superconducting qubits. The Josephson junction is denoted by the blue 'X'. **b–d**, Potential energy  $U(\Phi)$  (red) and qubit energy levels (black) for charge (**b**), flux (**c**), and phase qubits (**d**), respectively. **e–h**, Micrographs of superconducting qubits. The circuits are made of Al films. The Josephson

junctions consist of  $\text{Al}_2\text{O}_3$  tunnel barriers between two layers of Al. **e**, Charge qubit, or a Cooper pair box. **f**, Transmon, a derivative of charge qubit with large  $E_J/E_C$  (courtesy of R. J. Schoelkopf). The Josephson junction in the middle is not visible at this scale. **g**, Flux qubit (courtesy of J. E. Mooij). **h**, Phase qubit (courtesy of J. M. Martinis).

is defined by a Josephson junction. Qubits of this type were first developed<sup>71</sup> in the regime of  $E_J/E_C \ll 1$ , and later extended to  $E_J/E_C \gg 1$  and named 'quantronium'<sup>72</sup> and 'transmon'<sup>73</sup>. In the flux qubit<sup>74</sup>, also known as a persistent-current qubit, the circuit is designed to give a double-well potential. The two minima correspond to persistent currents going in opposite directions along the loop. Often the inductance is substituted by an array of Josephson junctions. The kinetic energy term is kept small, so  $E_J/E_C \gg 1$ . In the phase qubit<sup>75</sup>, the potential is biased at a different point and again  $E_J/E_C \gg 1$ , so that the phase qubit may use the two-lowest energy states in a single metastable anharmonic potential well.

Typically, the qubit excitation frequency is designed at 5–10 GHz, which is high enough to minimize thermal effects at the low temperatures available in dilution refrigerators ( $\sim 10$  mK;  $k_B T/h \approx 0.2$  GHz) and low enough for ease of microwave engineering. Single-qubit gates are implemented with resonant pulses of duration 1–10 ns, delivered to the qubit locally using on-chip wires.

Neighbouring qubits naturally couple to each other either capacitively or inductively, allowing simple quantum logic gates. However, for large-scale quantum computer architectures, more adjustable coupling schemes are desirable. Indirect couplings mediated by a tunable coupler have been developed for switching on and off the interaction between qubits<sup>76</sup>. The application of tunably coupled qubits to adiabatic quantum computing is also under investigation<sup>77</sup>.

Coupling qubits with microwave 'photons' in a transmission line has brought a new paradigm to superconducting quantum circuits. Transmission-line-based resonators have extremely small mode volumes and thus achieve cavities with strong cooperativity factors<sup>78</sup>. Such systems have allowed two-qubit gate operations within a few tens of nanoseconds and have been used for implementing algorithms<sup>79</sup> and for measurements of non-local quantum correlations<sup>80,81</sup> between qubits millimetres apart.

High-fidelity qubit readout schemes are under development. The switching behaviour of a current-biased Josephson junction at its critical current is commonly used as a threshold discriminator of the two qubit states<sup>80</sup>. Another promising development is the demonstration of QND measurements in which a qubit provides a state-dependent phase shift for an electromagnetic wave in a transmission line<sup>82</sup>. A high readout fidelity of  $\sim 95\%$  and a fast QND readout within tens of nanoseconds have been achieved.

A notable feature of superconducting qubits is their macroscopic scale: they involve the collective motion of a large number ( $\sim 10^{10}$ ) of conduction electrons in devices as large as  $100 \mu\text{m}$ . Common wisdom is that superpositions of these larger, more 'macroscopic' states should suffer faster decoherence than more 'microscopic' systems. However, the distressingly short decoherence times of a few nanoseconds observed in the earliest experiments have recently been

extended to  $T_1$  and  $T_2$  values of a few to several microseconds, now ten to a hundred times longer than the demonstrated initialization, read-out, and universal logic timescales. Nevertheless, understanding and eliminating the decoherence still remains the biggest challenge for superconducting qubits. Material engineering on the microscopic scale may be required to eliminate the remaining noise sources.

### Other technologies

A large number of other technologies exhibiting quantum coherence, besides those we have discussed above, have been proposed and tested for quantum computers.

As one example, the single photons in photonic quantum computers could be replaced by single, ballistic electrons in low-temperature semiconductor nanostructures, which may offer advantages in the availability of nonlinearities for interactions and in detection. As another emerging example, quantum computers based on ions and atoms may benefit from using small, polar molecules instead of single atoms, because the rotational degrees of freedom of molecules offer more possibilities for coherent control<sup>83</sup>.

Another solid-state system under investigation is that of rare-earth ions in crystalline hosts, whose hyperfine states have been known for many years to show long coherence times. Unfortunately, the weak optical transitions of these impurity ions prevent single-atom detection, and so, like nuclear-magnetic-resonance quantum computing, this approach employs an ensemble. The extremely high ratio of homogeneous to inhomogeneous broadening in such systems (typically 1 kHz versus 10 GHz for  $\text{Eu:YAlO}_3$ ) allows the resolution of as many as  $10^7$  qubits, defined as groups of ions with a well defined optical transition frequency isolated by a narrow-bandwidth laser. The initial state of rare-earth qubits can be initialized via optical pumping of hyperfine sublevels of the ground state<sup>84</sup>. Multi-qubit gates are possible via the large permanent dipole moment in both ground and excited electronic states. These qubits may provide an efficient interface between flying and matter qubits with storage times for photons of up to 10 s (ref. 85).

Other materials for hosting single-electron-based qubits are also under consideration. The carbon-based nanomaterials of fullerenes<sup>86</sup>, nanotubes<sup>87</sup> and graphene<sup>88</sup> have excellent properties for hosting arrays of electron-based qubits. Electrons for quantum computing may also be held in a low-decoherence environment on the surface of liquid helium<sup>89</sup>, or be contained in molecular magnets<sup>90</sup>.

A further category of exploration for quantum computation involves methods of mediating quantum logic between qubits, often of existing types. A key example of this is the use of superconducting transmission line cavities and resonators for qubits other than those based on Josephson junctions, such as ions<sup>91</sup>, polar molecules<sup>92</sup> and quantum dots<sup>93</sup>. Edge-currents in quantum-Hall systems present

another type of coherent current that may be useful for wiring quantum computers<sup>94</sup>. Nearly every type of bosonic field has been explored for quantum wiring, including lattice phonons in semiconductors<sup>95</sup>, phonons in micromechanical oscillators<sup>96</sup>, free excitons<sup>97</sup> or hybridizations between excitons and cavity photons in semiconductors<sup>98</sup>, and spin-waves in magnetic crystals<sup>99</sup>. Other ideas in this category include surface-acoustic waves for shuttling spin qubits<sup>100</sup> and plasmonic technologies for shuttling photonic qubits at sub-wavelength scales<sup>101</sup>.

A final, crucial development in quantum computation is the use of topologically defined quantum gates to preserve quantum information. Such concepts are used to define remarkably powerful fault-tolerant QEC schemes among ordinary qubits<sup>102</sup>, but have also been proposed as a method of physical computation should appropriate hardware be found. For example, a type of quantum excitation with fractional quantum statistics known as the ‘anyon’ has been predicted to play a part in condensed-matter systems. Implementing quantum logic by the braiding of such particles may offer more advanced future routes to robust quantum computation<sup>103</sup>.

## Outlook

Looking to the future, which type of hardware has the most promise for achieving a large-scale quantum computer? To answer this very difficult question, we might compare coherence times, as summarized in Table 1. These  $T_2$  times may improve as the technologies develop, and they vary by many orders of magnitude, with the largest given for trapped ions for one particular transition in one particular ion trap configuration. Each qubit’s  $T_2$ , however, must be compared to the timescales required to control, initialize and measure that qubit. Also, in practice, it may arise that imperfections in the coherent control of qubits are more likely to limit a computer’s performance than decoherence. Table 1 therefore also gives results of one-qubit and multi-qubit errors, to which decoherence during the gate time is but one contribution.

But Table 1 does not have nearly enough information to compare different potential technologies because the number of quantum gates, initializations and measurements depend critically on the form of QEC employed. Further, comparing methods of QEC is not as simple as examining a single number, such as the fault-tolerant threshold; one must also consider constraints for connectivity between qubits, the specific noise-processes for that hardware, and the relative speed of qubit-to-qubit communication, control, initialization and measurement.

In the end, a valuable comparison must examine complete architectures of quantum computers that enumerate the resources required to finish algorithms of relevant size with negligible error. As a result of the last couple of decades of quantum information science, the community may begin to seriously engage in designing and then comparing such architectures. Increased effort in this direction is needed to move towards realizing devices based on quantum principles that are actually more powerful, more efficient or less costly than their classical counterparts.

A large-scale quantum computer is certainly an extremely ambitious goal, appearing to us now as large, fully programmable classical computers must have seemed a century ago. However, as we approach this goal, we will grow accustomed to controlling the counterintuitive properties of quantum mechanics, and may reasonably expect side benefits such as new materials and new types of sensors. When we have mastered quantum technology enough to scale up a quantum computer, we will have tamed the quantum world and become inured to a new form of technological reality.

- Nielsen, M. A. & Chuang, I. L. *Quantum Computation and Quantum Information* (Cambridge University Press, 2000).
- Knill, E. Quantum computing with realistically noisy devices. *Nature* **434**, 39–44 (2005).
- DiVincenzo, D. P. The physical implementation of quantum computation. *Fortschr. Phys.* **48**, 771–783 (2000).

- Mizel, A., Lidar, D. A. & Mitchell, M. Simple proof of equivalence between adiabatic quantum computation and the circuit model. *Phys. Rev. Lett.* **99**, 070502 (2007).
- Raussendorf, R. & Briegel, H. J. A one-way quantum computer. *Phys. Rev. Lett.* **86**, 5188–5191 (2001).
- Cory, D. G., Fahmy, A. F. & Havel, T. F. Ensemble quantum computing by NMR-spectroscopy. *Proc. Natl Acad. Sci. USA* **94**, 1634–1639 (1997).
- Gershenfeld, N. A. & Chuang, I. L. Bulk spin resonance quantum computation. *Science* **275**, 350–356 (1997).
- Ryan, C. A., Moussa, O., Baugh, J. & Laflamme, R. Spin based heat engine: demonstration of multiple rounds of algorithmic cooling. *Phys. Rev. Lett.* **100**, 140501 (2008).
- Shor, P. W. & Jordan, S. P. Estimating Jones polynomials is a complete problem for one clean qubit. *Quant. Inform. Comput.* **8**, 681–714 (2008).
- Braunstein, S. L. & van Loock, P. Quantum information with continuous variables. *Rev. Mod. Phys.* **77**, 513–577 (2005).
- Schmidt, H. & Imamoglu, A. Giant Kerr nonlinearities obtained by electromagnetically induced transparency. *Opt. Lett.* **21**, 1936–1938 (1996).
- Duan, L. M. & Kimble, H. J. Scalable photonic quantum computation through cavity-assisted interactions. *Phys. Rev. Lett.* **92**, 127902 (2004).
- Knill, E., Laflamme, R. & Milburn, G. J. A scheme for efficient quantum computation with linear optics. *Nature* **409**, 46–52 (2001).
- Politi, A., Matthews, J. C. F. & O’Brien, J. L. Shor’s quantum factoring algorithm on a photonic chip. *Science* **325**, 1221 (2009).
- O’Brien, J. L. Optical quantum computing. *Science* **318**, 1567–1570 (2007).
- Migdall, A. & Dowling, J. (eds) Single-photon detectors, applications, and measurement. *J. Mod. Opt.* **51**, (2004).
- Hadfield, R. H. Single-photon detectors for optical quantum information applications. *Nature Photon.* **3**, 696–705 (2009).
- Grangier, P., Sandels, B. & Vuckovic, J. (eds) Focus on single photons on demand. *New J. Phys.* **6**, (2004).
- Shields, A. Semiconductor quantum light sources. *Nature Photon.* **1**, 215–223 (2007).
- Matthews, J. C. F., Politi, A., Stefanov, A. & O’Brien, J. L. Manipulation of multi-photon entanglement in waveguide quantum circuits. *Nature Photon.* **3**, 346–350 (2009).
- Bisler, C. et al. Demonstration of strong coupling via electro-optical tuning in high-quality QD-micropillar systems. *Opt. Express* **16**, 15006–15012 (2008).
- Fushman, I. et al. Controlled phase shifts with a single quantum dot. *Science* **320**, 769–772 (2008).
- Gruber, A. et al. Scanning confocal optical microscopy and magnetic resonance on single defect centers. *Science* **276**, 2012–2014 (1997).
- Devitt, S. J. et al. Photonic module: an on-demand resource for photonic entanglement. *Phys. Rev. A* **76**, 052312 (2007).
- Wineland, D. J. et al. Experimental issues in coherent quantum-state manipulation of trapped atomic ions. *J. Res. Natl. Inst. Stand. Technol.* **103**, 259–328 (1998).
- Wineland, D. & Blatt, R. Entangled states of trapped atomic ions. *Nature* **453**, 1008–1014 (2008).
- Ospelkaus, C. et al. Trapped-ion quantum logic gates based on oscillating magnetic fields. *Phys. Rev. Lett.* **101**, 090502 (2008).
- Garcia-Ripoll, J. J., Zoller, P. & Cirac, J. I. Speed optimized two-qubit gates with laser coherent control techniques for ion trap quantum computing. *Phys. Rev. Lett.* **91**, 157901 (2003).
- Leibfried, D., Blatt, R., Monroe, C. & Wineland, D. Quantum dynamics of single trapped ions. *Rev. Mod. Phys.* **75**, 281–324 (2003).
- Home, J. P. et al. Complete methods set for scalable ion trap quantum information processing. *Science* **325**, 1227–1230 (2009).
- Olmschenk, S. et al. Quantum teleportation between distant matter qubits. *Science* **323**, 486–489 (2009).
- Dür, W., Briegel, H. J., Cirac, J. I. & Zoller, P. Quantum repeaters based on entanglement purification. *Phys. Rev. A* **59**, 169–181 (1999).
- Duan, L.-M. & Raussendorf, R. Efficient quantum computation with probabilistic quantum gates. *Phys. Rev. Lett.* **95**, 080503 (2005).
- Morsch, O. & Oberthaler, M. Dynamics of Bose-Einstein condensates in optical lattices. *Rev. Mod. Phys.* **78**, 179–215 (2006).
- Anderlini, M. et al. Controlled exchange interaction between pairs of neutral atoms in an optical lattice. *Nature* **448**, 452–456 (2007).
- Urban, E. et al. Observation of Rydberg blockade between two atoms. *Nature Phys.* **5**, 110–114 (2009).
- Gaëtan, A. et al. Observation of collective excitation of two individual atoms in the Rydberg blockade regime. *Nature Phys.* **5**, 115–118 (2009).
- Negrevergne, C. et al. Benchmarking quantum control methods on a 12-qubit system. *Phys. Rev. Lett.* **96**, 170501 (2006).
- Vandersypen, L. M. K. et al. Experimental realization of Shor’s quantum factoring algorithm using nuclear magnetic resonance. *Nature* **414**, 883–887 (2001).
- Khaneja, N., Reiss, T., Kehlet, C., Schulte-Herbruggen, T. & Glaser, S. J. Optimal control of coupled spin dynamics: design of NMR pulse sequences by gradient ascent algorithms. *J. Magn. Reson.* **172**, 296–305 (2005).
- Braunstein, S. L. et al. Separability of very noisy mixed states and implications for NMR quantum computing. *Phys. Rev. Lett.* **83**, 1054–1057 (1999).
- Mehring, M., Mende, J. & Scherer, W. Entanglement between an electron and a nuclear spin 1/2. *Phys. Rev. Lett.* **90**, 153001 (2003).



43. Hanson, R., Kouwenhoven, L. P., Petta, J. R., Tarucha, S. & Vandersypen, L. M. K. Spins in few-electron quantum dots. *Rev. Mod. Phys.* **79**, 1217–1265 (2007).
44. Uhrig, S. G. Keeping a quantum bit alive by optimized  $\pi$ -pulse sequences. *Phys. Rev. Lett.* **98**, 100504 (2007).
45. Liu, H. W. *et al.* A gate-defined silicon quantum dot molecule. *Appl. Phys. Lett.* **92**, 222104 (2008).
46. Simmons, C. B. *et al.* Charge sensing and controllable tunnel coupling in a Si/SiGe double quantum dot. *Nano Lett.* **9**, 3234–3238 (2009).
47. Kane, B. E. A silicon-based nuclear spin quantum computer. *Nature* **393**, 133–137 (1998).
48. Vrijen, R. *et al.* Electron-spin-resonance transistors for quantum computing in silicon-germanium heterostructures. *Phys. Rev. A* **62**, 012306 (2000).
49. Tyryshkin, A. M. & Lyon, S. A. Data presented at the Silicon Qubit Workshop, 24–25 August (University of California, Berkeley; sponsored by Lawrence Berkeley National Laboratory and Sandia National Laboratory, 2009).
50. Ladd, T. D., Maryenko, D., Yamamoto, Y., Abe, E. & Itoh, K. M. Coherence time of decoupled nuclear spins in silicon. *Phys. Rev. B* **71**, 14401 (2005).
51. Yang, A. *et al.* Simultaneous subsecond hyperpolarization of the nuclear and electron spins of phosphorus in silicon by optical pumping of exciton transitions. *Phys. Rev. Lett.* **102**, 257401 (2009).
52. Batra, A., Weis, C. D., Reijonen, J., Persaud, A. & Schenkel, T. Detection of low energy single ion impacts in micron scale transistors at room temperature. *Appl. Phys. Lett.* **91**, 193502 (2007).
53. O'Brien, J. L. *et al.* Towards the fabrication of phosphorus qubits for a silicon quantum computer. *Phys. Rev. B* **64**, 161401 (2001).
54. Schneider, C. *et al.* Lithographic alignment to site-controlled quantum dots for device integration. *Appl. Phys. Lett.* **92**, 183101 (2008).
55. Atatüre, M. *et al.* Quantum-dot spin-state preparation with near-unity fidelity. *Science* **312**, 551–553 (2006).
56. Gerardot, B. D. *et al.* Optical pumping of a single hole spin in a quantum dot. *Nature* **451**, 441–444 (2008).
57. Press, D., Ladd, T. D., Zhang, B. Y. & Yamamoto, Y. Complete quantum control of a single quantum dot spin using ultrafast optical pulses. *Nature* **456**, 218–221 (2008).
58. Berezovsky, J. *et al.* Nondestructive optical measurements of a single electron spin in a quantum dot. *Science* **314**, 1916–1920 (2006).
59. Harrison, J., Sellars, M. J. & Manson, N. B. Measurement of the optically induced spin polarisation of N-V centres in diamond. *Diamond Related Mater.* **15**, 586–588 (2006).
60. Dutt, M. V. G. *et al.* Quantum register based on individual electronic and nuclear spin qubits in diamond. *Science* **316**, 1312–1316 (2007).
61. Neumann, P. *et al.* Multipartite entanglement among single spins in diamond. *Science* **320**, 1326–1329 (2008).
62. Jiang, L. *et al.* Repetitive readout of a single electronic spin via quantum logic with nuclear spin ancillae. *Science* **326**, 267–272 (2009).
63. Hanson, R., Dobrovitski, V. V., Feiguin, A. E., Gywat, O. & Awschalom, D. D. Coherent dynamics of a single spin interacting with an adjustable spin bath. *Science* **320**, 352–355 (2008).
64. Takahashi, S., Hanson, R., van Tol, J., Sherwin, M. S. & Awschalom, D. D. Quenching spin decoherence in diamond through spin bath polarization. *Phys. Rev. Lett.* **101**, 047601 (2008).
65. Balasubramanian, G. *et al.* Ultralong spin coherence time in isotopically engineered diamond. *Nature Mater.* **8**, 383–387 (2009).
66. Neumann, P. *et al.* Scalable quantum register based on coupled electron spins in a room temperature solid. *Nature Phys.* doi:10.1038/nphys1536 (in the press).
67. Wang, C. F. *et al.* Fabrication and characterization of two-dimensional photonic crystal microcavities in nanocrystalline diamond. *Appl. Phys. Lett.* **91**, 201112 (2007).
68. Wu, E. *et al.* Room temperature triggered single-photon source in the near infrared. *New J. Phys.* **9**, 434 (2007).
69. Wang, C., Kurtsiefer, C., Weinfurter, H. & Burchard, B. Single photon emission from SiV centres in diamond produced by ion implantation. *J. Phys. At. Mol. Opt. Phys.* **39**, 37–41 (2006).
70. Sanaka, K., Pawlis, A., Ladd, T. D., Lischka, K. & Yamamoto, Y. Indistinguishable photons from independent semiconductor nanostructures. *Phys. Rev. Lett.* **103**, 053601 (2009).
71. Nakamura, Y., Pashkin, Yu., A. & Tsai, J. S. Coherent control of macroscopic quantum states in a single-Cooper-pair box. *Nature* **398**, 786–788 (1999).
72. Vion, D. *et al.* Manipulating the quantum state of an electrical circuit. *Science* **296**, 886–889 (2002).
73. Schreier, J. A. *et al.* Suppressing charge noise decoherence in superconducting charge qubits. *Phys. Rev. B* **77**, 180502 (2008).
74. Chiorescu, I., Nakamura, Y., Harmans, C. J. P. M. & Mooij, J. E. Coherent quantum dynamics of a superconducting flux qubit. *Science* **299**, 1869–1871 (2003).
75. Martinis, J. M., Nam, S., Aumentado, J. & Urbina, C. Rabi oscillations in a large Josephson-junction qubit. *Phys. Rev. Lett.* **89**, 117901 (2002).
76. Niskanen, A. O. *et al.* Quantum coherent tunable coupling of superconducting qubits. *Science* **316**, 723–726 (2007).
77. Harris, R. *et al.* Experimental demonstration of a robust and scalable flux qubit. Preprint at (<http://arxiv.org/abs/0909.4321>) (2009).
78. Wallraff, A. *et al.* Strong coupling of a single photon to a superconducting qubit using circuit quantum electrodynamics. *Nature* **431**, 162–167 (2004).
79. DiCarlo, L. *et al.* Demonstration of two-qubit algorithms with a superconducting quantum processor. *Nature* **260**, 240–244 (2009).
80. Ansmann, M. *et al.* Violation of Bell's inequality in Josephson phase qubits. *Nature* **461**, 504–506 (2009).
81. Chow, J. M. *et al.* Entanglement metrology using a joint readout of superconducting qubits. Preprint at (<http://arxiv.org/abs/0908.1955>) (2009).
82. Lupascu, A. *et al.* Quantum non-demolition measurement of a superconducting two-level system. *Nature Phys.* **3**, 119–123 (2007).
83. Micheli, A., Brennen, G. K. & Zoller, P. A toolbox for lattice-spin models with polar molecules. *Nature Phys.* **2**, 341–347 (2006).
84. Rippe, L., Julsgaard, B., Walther, A., Ying, Y. & Kroll, S. Experimental quantum-state tomography of a solid-state qubit. *Phys. Rev. A* **77**, 022307 (2008).
85. de Riedmatten, H., Afzelius, M., Staudt, M. U., Simon, C. & Gisin, N. A solid-state light-matter interface at the single-photon level. *Nature* **456**, 773–777 (2008).
86. Morton, J. J. L. *et al.* Bang-bang control of fullerene qubits using ultrafast phase gates. *Nature Phys.* **2**, 40–43 (2006).
87. Mason, N., Biercuk, M. J. & Marcus, C. M. Local gate control of a carbon nanotube double quantum dot. *Science* **303**, 655–658 (2004).
88. Trauzettel, B., Bulaev, D. V., Loss, D. & Burkard, G. Spin qubits in graphene quantum dots. *Nature Phys.* **3**, 192–196 (2007).
89. Platzman, P. M. & Dykman, M. I. Quantum computing with electrons floating on liquid helium. *Science* **284**, 1967–1969 (1999).
90. Leuenberger, M. N. & Loss, D. Quantum computing in molecular magnets. *Nature* **410**, 789–793 (2001).
91. Tian, L., Rabl, P., Blatt, R. & Zoller, P. Interfacing quantum-optical and solid-state qubits. *Phys. Rev. Lett.* **92**, 247902 (2004).
92. Andre, A. *et al.* A coherent all-electrical interface between polar molecules and mesoscopic superconducting resonators. *Nature Phys.* **2**, 636–642 (2006).
93. Recher, P., Sukhorukov, E. V. & Loss, D. Andreev tunneling, Coulomb blockade, and resonant transport of nonlocal spin-entangled electrons. *Phys. Rev. B* **63**, 165314 (2001).
94. Privman, V., Vagner, I. D. & Kventsel, G. Quantum computation in quantum-Hall systems. *Phys. Lett. A* **239**, 141–146 (1998).
95. Smelyanskiy, V. N., Petukhov, A. G. & Osipov, V. V. Quantum computing on long-lived donor states of Li in Si. *Phys. Rev. B* **72**, 081304 (2005).
96. Harsh, L. & Zoller, P. Coupled ion-nanomechanical systems. *Phys. Rev. Lett.* **93**, 266403 (2004).
97. Piermarocchi, C., Chen, P., Sham, L. J. & Steel, D. G. Optical RKKY interaction between charged semiconductor quantum dots. *Phys. Rev. Lett.* **89**, 167402 (2002).
98. Quinteiro, G. F., Fernandez-Rossier, J. & Piermarocchi, C. Long-range spin-qubit interaction mediated by microcavity polaritons. *Phys. Rev. Lett.* **97**, 097401 (2006).
99. Khitun, A., Ostroumov, R. & Wang, K. L. Spin-wave utilization in a quantum computer. *Phys. Rev. A* **64**, 062304 (2001).
100. Barnes, C. H. W., Shilton, J. M. & Robinson, A. M. Quantum computation using electrons trapped by surface acoustic waves. *Phys. Rev. B* **62**, 8410–8419 (2000).
101. Chang, D. E., Sørensen, A. S., Hemmer, P. R. & Lukin, M. D. Quantum optics with surface plasmons. *Phys. Rev. Lett.* **97**, 053002 (2006).
102. Raussendorf, R. & Harrington, J. Fault-tolerant quantum computation with high threshold in two dimensions. *Phys. Rev. Lett.* **98**, 190504 (2007).
103. Nayak, C., Simon, S. H., Stern, A., Freedman, M. & Das Sarma, S. Non-abelian anyons and topological quantum computation. *Rev. Mod. Phys.* **80**, 1083–1159 (2008).
104. Langer, C. *et al.* Long-lived qubit memory using atomic ions. *Phys. Rev. Lett.* **95**, 060502 (2005).
105. Knill, E. *et al.* Randomized benchmarking of quantum gates. *Phys. Rev. A* **77**, 012307 (2008).
106. Benhelm, J., Kirchmair, G., Roos, C. F. & Blatt, R. Towards fault-tolerant quantum computing with trapped ions. *Nature Phys.* **4**, 463–466 (2008).
107. Treutlein, P., Hommelhoff, P., Steinmetz, T., Hänsch, T. W. & Reichel, J. Coherence in microchip traps. *Phys. Rev. Lett.* **92**, 203005 (2004).
108. Ryan, C. A., Laforest, M. & Laflamme, R. Randomized benchmarking of single- and multi-qubit control in liquid-state NMR quantum information processing. *New J. Phys.* **11**, 013034 (2009).
109. Bertet, P. *et al.* Dephasing of a superconducting qubit induced by photon noise. *Phys. Rev. Lett.* **95**, 257002 (2005).
110. Emerson, J. *et al.* Symmetrized characterization of noisy quantum processes. *Science* **317**, 1893–1896 (2007).
111. Hanson, R., Awschalom, D. D. Coherent manipulation of single spins in semiconductors. *Nature* **453**, 1043–1049 (2008).

**Acknowledgements** We thank R. Hanson, M. D. Lukin, and W. D. Oliver for comments. We acknowledge support from NSF, EPSRC, QIP IRC, IARPA, ERC, the Leverhulme Trust, CREST-JST, DFG, BMBF and Landesstiftung BW. J.L.O'B. acknowledges a Royal Society Wolfson Merit Award.

**Author Contributions** All authors contributed to all aspects of this work.

**Author Information** Reprints and permissions information is available at [www.nature.com/reprints](http://www.nature.com/reprints). The authors declare no competing financial interests. Correspondence should be addressed to J.L.O'B. ([jeremy.obrien@bristol.ac.uk](mailto:jeremy.obrien@bristol.ac.uk)).